

SMOKE DETECTOR PLACEMENT IN COMPARTMENTS WITH HONEYCOMB CEILING A Numerical Study

by

**Darko N. ZIGAR^a, Milan Dj. BLAGOJEVIĆ^{a*}, Dušica J. PEŠIĆ^a,
Aca V. BOŽILOV^b, and Vlastimir D. NIKOLIĆ^b**

^a Faculty of Occupational Safety, University of Niš, Niš, Serbia

^b Faculty of Mechanical Engineering, University of Niš, Niš, Serbia

Original scientific paper

<https://doi.org/10.2298/TSCI220819205Z>

One of the most interesting problems in fire detection system design is the problem referred to as detector position on a 'honeycomb ceiling', because beams and joists affect stratification of smoke and, consequently, smoke detector response time. The aim of this paper is to determine optimal smoke detector placement – on the underside of beams or on the structural slab in the cells. On the basis of rules of standards for smoke detector location, the large eddy simulation method of fire dynamics simulator software package was employed to investigate the effects of 'honeycomb' density on smoke detector response time. The simulation results show that the columns, beams, joists and similar structural elements affect stratification of smoke and, consequently, smoke detector response time. In the case when the honeycomb cells are small, the detectors on the underside of the beams react faster because the smoke does not enter the cells in sufficient quantity to activate the optical smoke detector located on the structural plate in the cells that form the beams. On the basis of the obtained results, a satisfactory solution for most possible situations that could occur in practice has been proposed.

Key words: honeycomb ceiling, fire detection, fire dynamics simulator, simulation, smoke detector location

Introduction

In practical engineering applications, different types of beam structures are widely used, because they can optimize weight and change strength by changing the cross-sectional area and material properties. Uniform and non-uniform beams, sandwich composite structures, and honeycomb structures are increasingly used in many fields of engineering and practically always used as structural elements [1, 2].

The structures with vertical and horizontal irregularity and cross bracing can be found not only in almost all large built industrial environments but also in shopping malls, transportation hubs, exhibition centers and tall residential and commercial buildings.

Cross bracing is a system utilized to reinforce building structures in which diagonal supports intersect. This system is usually seen with two diagonal supports placed in an X-shaped manner or with joists at an angle of 90° and it can be applied to any rectangular frame structure. Cross bracing between joists or rafters strengthens the members by preventing side-

* Corresponding author, e-mail: milan.blagojevic@zrnrfak.ni.ac.rs

ways deflection. In regular light-frame construction and conventional roof framing, the ceiling is constructed using an arrangement of timber (or metal and concrete) joists and beams that run across the length and width of the ceiling [3]. Joists and beams create the ceiling of a room, and support the ceiling cladding (the part that is visible). Ceiling voids are deemed as concealed spaces in a built environment because they are often isolated or obstructed from view.

The response of beam structures under different external loads is very important from the aspect of their stability. Based on the type of loading, various buckling forms could occur, which can be global or local [4, 5].

Many researchers investigated beam properties at elevated temperature. Zhang *et al.* [6] focused on the temperature, displacement and stress analysis of simply-supported laminated beams with temperature-dependent material properties subjected to thermal and mechanical loads. The analysis revealed that the temperature not only produces deformations and stresses itself, but also affects the deformations and stresses induced by mechanical loads. Hu and Wang [7] created a thermal-mechanical analysis model to characterize thermal shock behaviors of auxetic honeycomb core ceramic sandwich structures. Safaei *et al.* [2] investigated the bending and critical buckling loads of a sandwich beam structure subjected to thermal load and axial compression using ANSYS software. Numerical results of thermal stresses and buckling temperature of the sandwich beam were validated analytically.

However, the building structures and materials are often exposed to very high temperatures that occur during fires. Namely, fire thermal load affects the properties of structure materials. Razdolsky [8] investigated the temperature-dependent modulus of elasticity and time-dependent creep data of materials at a given temperature in different fire scenarios. The predicted stress-strain curves can be used in structural analysis and building design.

In fire conditions, released heat affects the heating of the structural elements of the building structure, causing their damage [9]. Depending on the type of structure, the first damage to the structure begins as early as 300 °C, for example, with the reinforced concrete structure [10]. The load during the heating process has significant impacts on the mechanical properties of concrete at high temperatures [11]. The shear strength is one of the major components of the concrete mechanical properties and it plays a significant role in the overall behavior and failure of the concrete members. Moghadam and Izadifard [12] investigated the shear strength of concrete at temperatures in the range of 100-800 °C and concluded that with an increase in temperature, the shear strength of the concrete decreases and with further increase in temperature to 450 °C, the shear strength is restored, after which it begins to decline sharply.

The high fire temperatures cause deteriorations on structural elements and can greatly reduce the load-bearing capacity of load-bearing elements [13, 14]. The traditional approach to fire protection is based on coating with insulating material, which not only slows down construction but also increases costs. Installation of a fire detection system can significantly reduce these costs.

However, there are no rules in the standards for fire detection system design for all types of constructions, especially for the cross-bracing system that is utilized to reinforce building structures. From a fire detection point of view, voids formed by joists and beams complicate fire detection system design [15]. If a fire originating in compartments with a concealed space is detected too late or encountered with inadequate response measures, the resulting damage can be substantial. Five world leading standards – American – NFPA 72, European – EN 54-14, German – VDE 0833-2, British – BS 5839, and Russian – SP 484.1311500 – deal with this problem in more or less detail in the way described in this paper.

These facts provide enough reasons to investigate the problem of fire detection on honeycombs as a special form of ceiling irregularity [16]. Because of the aforementioned facts related to rules in various standards, initial investigation assumptions made in this paper were taken from the standards. On the basis of the assumptions, smoke detector response was numerically modelled. Fire dynamics simulator (FDS), *i.e.*, PyroSim as an integrated development environment, was used to select the optimal solution for installing detectors on a building's honeycomb ceiling.

Rules and recommendations for smoke detector location

As mentioned previously, the leading world standards state the rules for the honeycomb problem differently. Within its basic rules for smoke detector sitting, European standard EN 54-14 takes into consideration internal volumes of cells covered by a single detector. According to this standard, a single point thermal or smoke detector may cover a group of cells. When a smoke detector is used, the internal volume of cells covered by the single detector should not exceed the value:

$$TCV = 12(H - h) \quad (1)$$

where TCV is the total cell volume, H – the height of a compartment, and h – the depth of beams, A.6.4.1.f [17].

Rules in German standard DIN VDE 0833-2 are based on areas of ceiling bays formed by subdividing elements. If the areas separated by beams have a surface that covers 60% or more of the maximum monitoring area A of a detector, *i.e.*, $0.6 \times A$, each ceiling bay shall be equipped with a detector, and if the area of the ceiling bay is $\leq 0.6 \times A$, then one detector can be used for monitoring several bays with a surface of no more than $1.2 \times A$, 6.2.7.4 [18].

British standard BS 5839-1 points out the relation between dimensions of cells, beam depth D and distance between beams W . Depending on those dimensions, detector location may be on the underside of beams if W is $4D$ or less, or on the structural slab in the cell if W is more than $4D$, tab. 1 [19].

Similarly, NFPA 72 standard states that if the ratio of beam depth, D , to ceiling height, H , (D/H) is greater than 0.10 and if the ratio of beam spacing, W , to ceiling height H (W/H) is greater than 0.40, detectors should be located in each beam pocket. If either the ratio of beam depth to ceiling height D/H is less than 0.10 or the ratio of beam spacing to ceiling height W/H is less than 0.40, detectors should be installed at the bottom of the beams, A.17.6.3.3 [20].

There are no special rules for ceiling irregularities such as the honeycomb structure in Russian standard CII 484.1311500 (former HIIБ 88). Instead, the honeycomb form is treated through the relation between the height of the ceiling and the depth of the joist, or by absolute values of the dimensions of beams that form this structure, 14.3.8 [21].

Obviously, there are two problems related to smoke detector sitting in presence of this type of ceiling irregularity: position of detectors and distance between detectors depending on the dimensions of joists and beams.

Numerical study

This research was carried out using the FDS open-source software package, developed by the National Institute of Standards and Technology. Since the FDS is a model of fire-driven fluid-flow, it numerically solves a form of the Navier-Stokes equations approximated for low speed and thermally-driven fluids. The governing equations are eqs. (2)-(5) [22]:

– Conservation of mass:

$$\frac{\partial \rho}{\partial t} + \nabla \rho \mathbf{u} = \dot{m}_b''' \quad (2)$$

which is often written in terms of the mass fractions of the individual gaseous species:

$$\frac{\partial}{\partial t}(\rho Y_\alpha) + \nabla \rho Y_\alpha \mathbf{u} = \nabla \rho D_\alpha \nabla Y_\alpha + \dot{m}_\alpha''' + \dot{m}_{b,\alpha}''' \quad (3)$$

– Conservation of momentum:

$$\frac{\partial}{\partial t}(\rho \mathbf{u}) + \nabla \rho \mathbf{u} \mathbf{u} + \nabla p = \rho \mathbf{g} + \mathbf{f}_b + \nabla \tau_{ij} \quad (4)$$

– Transport of sensible enthalpy:

$$\frac{\partial}{\partial t}(\rho h_s) + \nabla \rho h_s \mathbf{u} = \frac{Dp}{Dt} + \dot{q}''' - \dot{q}_b''' - \nabla \dot{q}'' + \varepsilon \quad (5)$$

where ρ is the density, \mathbf{u} – the three components of velocity ($= [u, v, w]^T$), T – the temperature, D_α – the diffusion coefficient, Y_α – the mass fraction of α^{th} species, $\dot{m}_{b,\alpha}'''$ – the production of species α by evaporating particles, p – the pressure, \mathbf{g} – the acceleration of gravity, \mathbf{f}_b – the external force vector, τ_{ij} – the stress tensor, h_s – the sensible enthalpy, \dot{q}''' – the heat release rate per unit volume from a chemical reaction, \dot{q}_b''' – the energy transferred to the evaporating droplets, \dot{q}'' – the conductive and radiation heat fluxes, ε – the dissipation rate, and t – the time.

The governing equations can be treated as large eddy simulation (LES) method or direct numerical simulation (DNS). Since the focus of this paper is on the thermal flow of smoke, which is conditioned by its *buoyancy*, the FDS LES method was used for numerical simulation response of smoke detectors depending on their location – inside or outside of joists.

Theoretical background

The starting point in making a decision related to ceiling irregularity dimensions for this numerical study was the choice of beam depth. The European standard states that any ceiling irregularity having a depth greater than 5% of the ceiling height should be treated as a wall [17]. The German standard specifies that elements subdividing the ceiling of a height of more than 3% of the room height are obstacles [18]. In the British standard, ceiling obstructions such as beams should be treated as walls if deeper than 10% of the ceiling height [19]. Similarly, NFPA 72 states 10% as the limit value, because for ceilings with beam depths of less than 10% of the ceiling height ($0.1 \times H$), smooth ceiling spacing shall be permitted [20]. Finally, the Russian standard recommends putting the point smoke detectors in each segment of the ceiling that is wider than 0.75 m if the depth of the joists exceeds 0.4 m [21].

Taking into account the said basic rules related to dimensions of joists, which have an effect on smoke stratification, a fire compartment with ceiling construction as shown in fig. 1 was chosen, with the following dimensions: ceiling height $H = 6.0$ m, beam depth $D = 0.3$ m and distance from beams $W = 1.2$ m, and $W = 2.4$ m, *i.e.*, $W = 4 \times D$ and $W = 8 \times D$, respectively.

There are several reasons for choosing these values. Beam depth of 0.3 m is equal to 5% of ceiling height and represents a limit value in EN 54-14. Because of that, after defining detector locations, it is necessary to calculate the value of TCV covered by a single detector.

According to this standard, a single point-type smoke detector may cover a group of cells if its internal volume does not exceed the value $V = 12 \text{ m}^2 \times (H - h)$, where H is the height of the ceiling and h is the depth of the beam of joist. Value D exceeds the 3% mentioned in the German standard, so after smoke detector placement it is necessary to calculate the value $0.6 \times A$ of the ceiling bays covered by a single smoke detector.

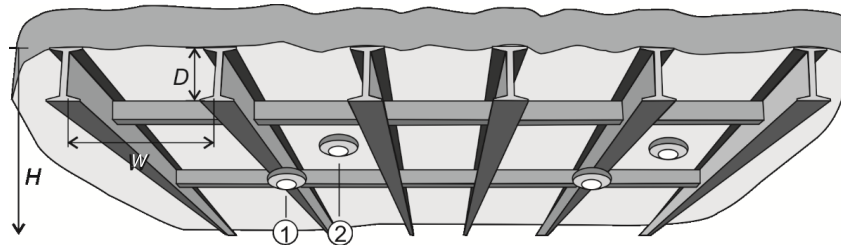


Figure 1. Positions of detectors

Finally, the relationship between $W = 4 \times D$, which is a limit value according to the British standard, and $W = 8 \times D$ (or $W > 4 \times D$) necessitates that detectors be put in pair at about the same distance from the fire source, *i.e.*, on the underside of the beams and on the structural slab in the cell (Positions 1 and 2 in fig. 1) in order to analyze the influence of the honeycomb structure on fire detection. These values satisfied the first two conditions from the British standard, tab. 1 [19].

Table 1. Rules from the British standard for maximum distance between smoke detectors

Ceiling height, H	Beam depth, D	Maximum distance	$W \leq 4 \times D$	$W > 4 \times D$
6 m or less	Less than 10% H	As per flat ceiling	Position 1	Position 2
More than 6 m	Less than 10% H and 600 mm or less	As per flat ceiling	Position 1	Position 2

Simulation set-up

In order to perform the numerical experiment of detector position on a *honeycomb ceiling*, it is necessary to define a model of building structure affected by fire, computational cell size, location of the fire source, fuel type, heat release rate and specific fire scenarios. In a computational domain (10.8 m wide, 21.6 m long, and 6.2 m high), the fire compartment was designed for CFD LES simulations. The compartment ceiling was built from the honeycomb structure, *i.e.*, joists with width and depth of 0.3 m.

For achieving the optimal solution for installing a smoke detector on the ceiling, numerical simulations were carried out for two cases:

- Scenario 1: Dimensions of every ceiling cell are 1.2 m \times 1.2 m \times 0.3 m with internal volume of $TCV = 0.432 \text{ m}^3$ and area of $S = 1.44 \text{ m}^2$, fig. 2(a).
- Scenario 2: Dimensions of cells are doubled: 2.4 m \times 2.4 m \times 0.3 m with internal volume of $TCV = 1.728 \text{ m}^3$ and area of $S = 5.76 \text{ m}^2$, fig. 2(b).

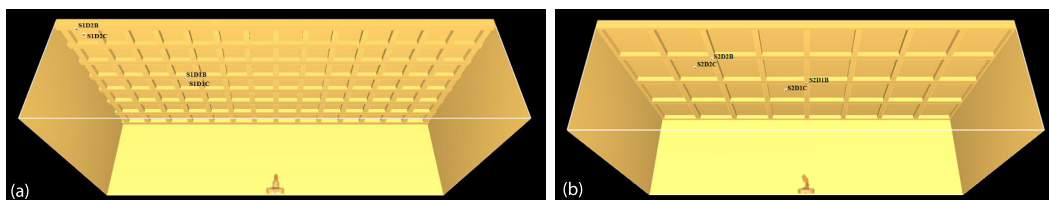


Figure 2. Simulation model; (a) Scenario 1 and (b) Scenario 2

Since the area of fire compartment is 233.28 m^2 , in accordance with all standards, four smoke detectors are required for total coverage. However, for the purpose of this investigation, a small modification has been made. Namely, the first pair of smoke detectors (located

on the underside of the beam and on the slab of the cell) is located a little outside the radii allowed by the European and German standards. The second pair of smoke detectors is located on the corner of the fire compartment, which is not applicable in practice, but in this case such arrangement of detectors allows the 'measurement' of time delay for detector responses. The distances between detectors in pairs on the beam and on the slab are approximately 0.4 m for both scenarios. The distances between the fire source and individual detectors are given in tab. 2. The detector marks are in the form XD1Y and XD2Y, where X = S1 and X = S2 denote the first and the second simulation, respectively. For both simulations, the detector pair closer to the fire is marked D1 and the detector pair in the corner is marked D2. Finally, suffix Y = B indicates detectors located on the underside of the beam, and Y = C indicates detectors located in the cell.

Table 2. Distances of detectors from fire for both scenarios

Scenario 1		Scenario 2	
S1D1C	8.294 m	S2D1C	7.059 m
S1D1B	8.698 m	S2D1B	7.479 m
S1D2C	14.385 m	S2D2C	10.901 m
S1D2B	14.851 m	S2D2B	10.956 m

Polyurethane G27 ($C_{25}H_{42}O_6N_2$) with critical flame temperature of 1327.0 °C was set as the fire buoyancy source (1.0 m × 1.0 m × 0.5 m) at the floor of the compartment. The assumption is that fire compartment under simulation is the storage space and that the coating on the beams burns first. According to the FDS reaction database [22], a reaction type of *Polyurethane* with soot yield = 0.198 and CO yield = 0.042 was specified for generating smoke and combustion products from the fire source. The

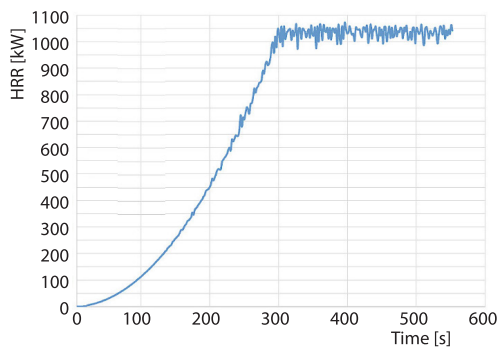


Figure 3. The HRR

growth phase of the fire was specified by the *t* square fire growth model [20]. Medium fire with growth coefficient of 0.01172 kW/s² was used for the simulations. Taking into account the initial incubation period in which thermal decomposition of the polyurethane occurred, the specified heat release rate (HRR) of 1055 kW was reached in 300 seconds and then maintained at 1055 kW constantly, fig. 3. The features of computer used for simulation is CPU Intel(R) Core (TM) i7-3770K, 3.50 GHz, 4 cores, 4 threads, 16 GB ram, 1 GB HDD.

Model validation

Before the simulation, it is necessary to check the validity of the numerical model in accordance with the requirements of the standards for smoke detector location. Since detector distances from the fire source for both models are known, it is necessary to calculate internal volume and surfaces of ceiling bays covered by detector radius of 7.5 m (according to EN 54-14) and 5.3 m (according to VDE 0833-2) [17, 18]. The number of covered cells, internal volume *TCV* and values $0.6 \times A$ covered by the detector nearest to fire for both scenarios are given for EN 54-14 criteria and for VDE 0833-2 criteria in tabs. 3 and 4, respectively.

Table 3. Internal volume of cells covered by a single detector

EN 54-14 criteria	Cells	TCV	Allowed
Scenario 1	49	21.16 m ³	68.4 m ³
Scenario 2	15	25.92 m ³	68.4 m ³

Table 4. Total area of cells covered by a single detector

VDE 0833-2 criteria	Cells	0.6 × A	Allowed
Scenario 1	25	30.24 m ²	36 m ²
Scenario 2	6	34.56 m ²	36 m ²

Tables 3 and 4 show that all parameters satisfied the maximal allowed criteria from the European and German standards for ceiling irregularity, which are designed according to the British standard.

On the other hand, to validate the numerical model, it is very important to determine the acceptable response range of the detector. It is known that manufacturers set alarm thresholds for point type smoke detectors by obscuration measured in [% per m], while for line type detectors the alarm threshold is defined by absolute obscuration in [%]. Consequently, it is necessary to take into consideration the recommended alarm thresholds from UL 268 [23], or more precisely, smoke detector test acceptance criteria for different colored smoke. According to this, the acceptable response range of the detector is 1.6-12.5% per m and 5.0-29.2% per m for grey and black smoke, respectively, NFPA 72, table B.4.7.4.2, [20]. Therefore, the value of 5% per m was accepted as the criterion for model validation, tab. 5.

Table 5. Number of cells and time for reaching the obscuration of 5% per m

Mesh size [m]	Time to 5% per m [second]	Number of cells
0.08	96.8	2765224
0.1	95.7	1446336
0.12	83.75	826200
0.15	87.9	425088
0.17	94.12	294912
0.2	80.2	180792
0.22	80.85	124416
0.25	81	92450

Since the accuracy of the numerical model largely depends on the mesh size, it was necessary to determine the optimal mesh resolution. The validation of the model was carried out for different mesh dimensions from 0.08-0.25 m and the time needed to achieve the obscuration of 5% per m was observed. The results of these simulations are shown in tab. 5 and the corresponding convergence curve, which represents the sufficient number of cells for simulations, is shown in fig. 4.

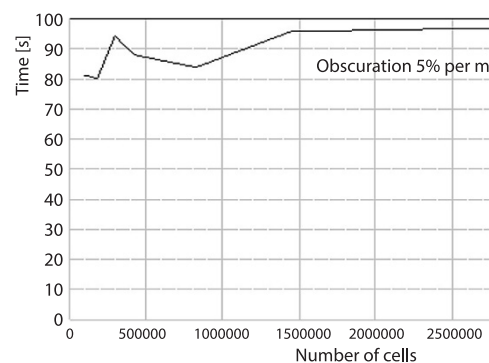


Figure 4. Convergence curve

Figure 4 shows that the mesh size of 0.1 m is sufficient to obtain reliable results. In other words, net *density* with the number of cells above 1500000 does not significantly affect the simulation results.

Results and discussion

To determine the optimal position of smoke detectors, the spread of fire products in a compartment was simulated first in this study. The results of stratification effect of smoke on the honeycomb structure in the time instance of 54.0 seconds of the simulations are shown in fig. 5 for both scenarios.

The obtained results show that fire flame and smoke plume rise in the form of convective current above the fire source and they are carried by a strong buoyancy force. The buoyancy force occurs due to the large quantity of heat released during the fire, leading to a strong thermal effect. It arises as a result of high temperature and low density of fire products compared to ambient air. It forces the gaseous products with high velocity directly upwards. Under these circumstances, by moving upward in the compartment, the smoke quickly fills its upper part. After that, its flow is restricted by the compartment ceilings. The fire-induced smoke plume flows horizontally near the ceilings forming the ceiling jet.

From the point of view of fire detection, the phenomenon of ceiling jet formation by fire products is very important. The jet is the rapid flow of gaseous combustion products in a thin layer just below the surface of the ceiling, which is caused by the buoyancy force of the heated gaseous products of the fire. Observing the movement of smoke under the ceiling, it can be noticed that their distance decreases with the distance from the fire source, because it cools down as it mixes with the surrounding air.

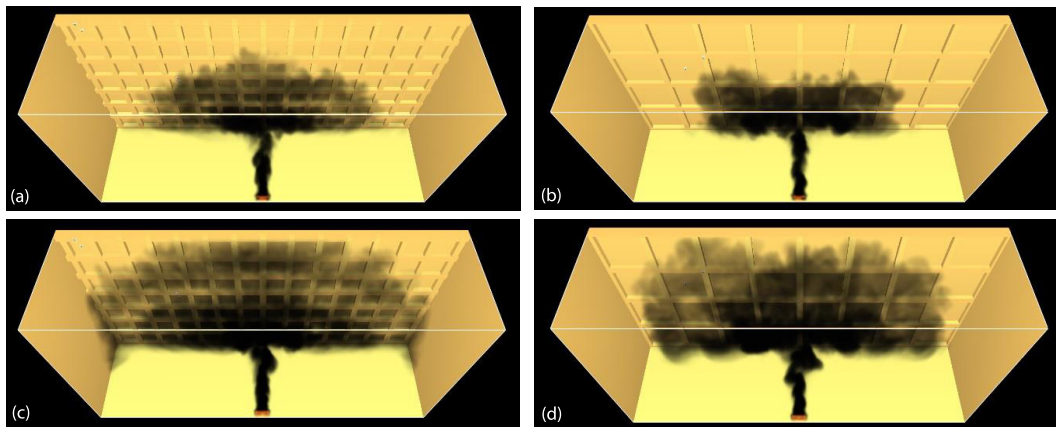


Figure 5. Smoke stratification effect on *honeycomb* structure: Scenario 1 in 54th second (a) and Scenario 2 in 70th second (b)

As shown in fig. 5, in the 1st scenario the stratification layer is wider but thinner at the given time instance, while in the second scenario this layer is narrower and thicker. Obviously, this happens as a consequence of the distance between the beams, because in the first scenario the smoke is dispersed over a larger area. In this time instance the measured obscuration on all detectors is 0% per m.

However, in the 2nd scenario (2.4 m distance between beams) the obscuration on the pair of detectors closer to the fire, *i.e.*, detectors S2D1C and S2D1B, is 6.87% per m and 23.01% per m, respectively. These values can be detected by point or line type smoke detectors.

This fact is confirmed by the curves of total obscuration for both scenarios shown in fig. 6. Obviously, the dimensions of the honeycomb affect the *filling* of the compartment by smoke.

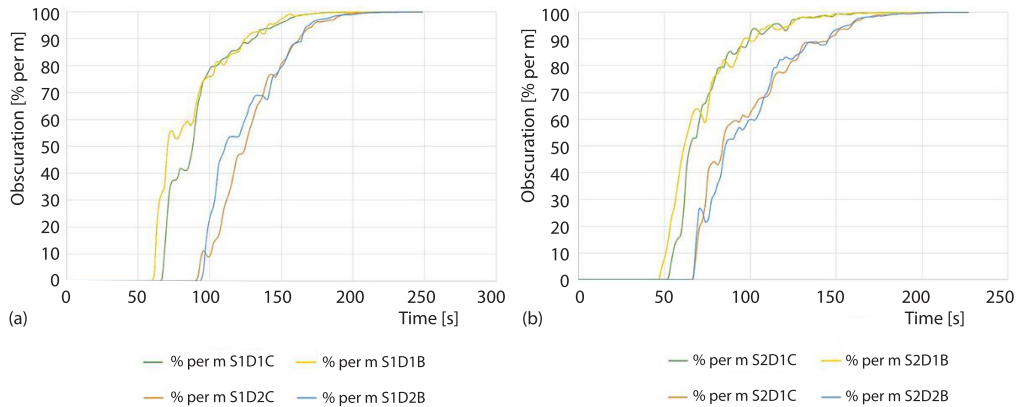


Figure 6. Obscuration; (a) Scenario 1 and (b) Scenario 2 (for color image see journal web site)

The distances between detectors in pairs on the beam and on the slab are approximately 0.4 m for both scenarios and consequently do not affect the conclusions related to response time. As mentioned earlier, the recommended alarm threshold of 5% per m is most often chosen for most environments, so the results for obscuration vs. time were extracted up to the obscuration of 20% per m for both scenarios, fig. 7.

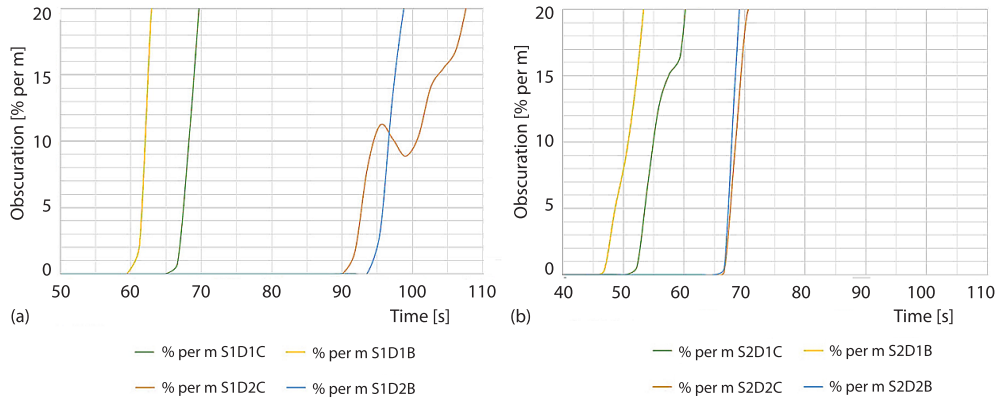


Figure 7. Obscuration; (a) Scenario 1 and (b) Scenario 2 (for color image see journal web site)

Two conclusions can be drawn immediately from the curves shown in fig. 7. The first conclusion is that detection time is shorter as dimension of the cells increase. Also, as detector distance from fire increases, the response times of the detector on the beam and in the cell become approximately the same. The second conclusion is that by reducing the dimensions of the cells, the detector on the underside of the beam will undoubtedly react faster than the detector on the structural slab.

Since early detection and consequently early warning is a priority upon fire occurrence, especially for timely evacuation, tabs. 6 and 7 show the characteristic values of obscuration that are important for fire detection. Table 6 contains the obscuration values for a beam spacing of 120 cm. For the pair of detectors closer to the fire, the obscuration on the beam and inside the honeycomb is almost equalized after 25 seconds, and after a few seconds the values of the obscuration are almost identical.

In the worst-case scenario, when the detector pair is at the maximum distance from the fire that is allowed by the European and German standards, the concentrations of smoke measured on the pair of detectors located closer to the fire are reached with a delay of a little over 30 seconds. The initial obscuration in terms of detection is almost the same, but there is a quick increase of obscuration on the beam in about 10 seconds, while at the same time the obscuration on the detector pair closer to the fire reaches the values between 75% per m and 82% per m. Finally, the concentration of smoke on the detectors located inside the cell reaches the values measured on the detectors mounted on the beam with a delay of about 7-8 seconds.

Table 6. Scenario 1 – Characteristic values of obscuration

Time [second]	Obscuration [% per m]		Time [second]	Obscuration [% per m]	
	S1D1C	S1D1B		S1D2C	S1D2B
63.01	0.00	20.52	97.21	10.16	13.56
64.82	0.00	29.58	99.00	8.88	20.79
66.61	0.77	32.75	100.81	10.31	25.11
68.41	11.10	35.09	102.60	14.09	27.78
70.21	23.65	48.37	104.40	15.50	34.10
72.00	34.09	55.15	106.21	16.93	43.16
73.81	37.12	55.72	108.01	21.15	46.02

Table 7. Scenario 2 – Characteristic values of obscuration

Time [second]	Obscuration [% per m]		Time [second]	Obscuration [% per m]	
	S2D1C	S2D1B		S2D2C	S2D2B
52.21	0.60	15.01	68.40	9.48	14.58
54.01	6.87	23.01	70.22	19.17	26.50
55.81	12.63	27.54	72.01	22.00	25.59
57.60	15.18	35.17	73.81	28.68	21.51
59.40	16.58	43.05	75.60	40.93	22.67
61.21	26.46	49.23	77.41	43.43	29.94
63.00	42.66	53.78	79.20	44.06	32.13
64.80	49.62	58.10	81.01	42.95	35.93
66.60	52.82	62.33	82.80	45.58	39.05
68.40	53.07	63.82	84.60	53.36	47.43

In Scenario 2, when the distance between the beams on the ceiling is twice as large – 240 cm – the values of obscuration on both detector pairs are reached 10-20 seconds earlier than when the distance between the beams is 120 cm. For example, values of 50% per m on the pair of detectors closer to the fire are reached 22 seconds earlier, tab. 7. However, the values on the furthest pair of detectors at this distance in relation to the pair at the distance of 120 cm between beams at the same location are reached earlier by more than half a minute, *i.e.*, in 36 seconds.

Although the value $W = 4 \times D$ appears in the British and American standards as the limit value below which the detector should be placed on the beam rather than inside the cell, it should still be considered whether this rule should always be applied to some applications.

The obtained simulation results showed that in both scenarios the smoke detector on the underside of the beam responds faster, especially if the honeycomb cells are small, because the combustion products do not enter the cells in sufficient quantity and do not create a sufficient concentration activate the optical smoke detector.

The difference in detector activation time is greater as the detector is placed closer to the fire source, and this difference decreases as the distance from the fire increases. Therefore, the approach from the German standard is more accurate, because it gives a better response than the 7.5 m rule specified by the European standard, without the problem that there can be redundancy in detector distribution.

Conclusions

The CFD simulations were carried out within the framework of studying the detector position on a honeycomb ceiling of a building with the aim of detecting a fire at an early stage. The FDS LES method was utilized to investigate the effects of honeycomb density on smoke detector response time. The main conclusions are as follows.

- The columns, beams, joists and similar structural elements affect stratification of smoke and, consequently, smoke detector response time.
- In the case when the honeycomb cells are small, the detectors on the underside of a beam react faster, because the smoke does not enter the cells in sufficient quantity to activate the optical smoke detector located on the structural plate in the cells that form the beams.
- For honeycombs with dimensions $W = 8 \times D$ and larger, the difference in response time of the detector is reduced.
- The obtained results show that some standards have satisfactorily solved the problem of fire detector location. The approach from the German standard is more accurate because it gives a more optimal response than the 7.5 m rule specified by the European standard, without the problem of potential redundancy in detector distribution.

Taking into account that many types of beams and joists are used for construction nowadays, it is recommended that a similar kind of simulation is performed if there is a plan to install a fire detection system. The cost of this system is very low in relational construction costs, but it reduces the risks incurred by fires in their developed phase.

Obviously, the systems of fire protection of the honeycomb structure require more research. The main reason for this is the response time of detectors, which directly influences the beginning of evacuation and fire extinguishment. In this study, numerical simulations were performed for a compartment height of 6 m, so the rules mentioned in this study should be verified further for lower or higher rooms. Since the simulations showed that the arrangement of ceiling irregularities significantly affects smoke stratification, the use of linear smoke detectors should also be considered. By using this type of detectors, it is possible to detect a fire immediately before the stratification layer is formed. On the other hand, there are also reasons of aesthetic nature, because detectors within the field are hidden from view and do not disturb the appearance of the interior of the compartment. The quantification of all those aspects could be a subject for further research.

Acknowledgment

This research is supported by the Ministry of Science and Technological Development of the Republic of Serbia (contract No. 451-03-68/2022-14/ 200148).

References

- [1] Wang, P., et al., Study on Vibration Response of a Non-Uniform Beam with Non-Linear Boundary Condition, *Facta Universitatis Series: Mechanical Engineering*, 19 (2021), 4, pp. 781-804
- [2] Safaei, B., et al., Thermal Buckling and Bending Analyses of Carbon Foam Beams Sandwiched by Composite Faces under Axial Compression, *Facta Universitatis Series: Mechanical Engineering*, 20 (2022), 3, pp. 589-615
- [3] Sewell, J., High Speed Cost Efficient Honeycomb Core Process Technology Bringing Innovation in Building Materials and Applications, *Reinforced Plastics*, 61 (2017), 6, pp. 335-338
- [4] Hu, H., et al., A Novel Finite Element for Global and Local Buckling Analysis of Sandwich Beams, *Composite Structures*, 90 (2009), 3, pp. 270-278
- [5] Wang, D., Abdalla, M. M., Global and Local Buckling Analysis of Grid-Stiffened Composite Panels, *Composite Structures*, 119 (2015), Jan., pp. 767-776
- [6] Zhang, Z., et al., Analysis of Laminated Beams with Temperature-Dependent Material Properties Subjected to Thermal and Mechanical Loads, *Composite Structures*, 227 (2019), 1113304
- [7] Hu, J. S., Wang, B. L., Crack Growth Behavior and Thermal Shock Resistance of Ceramic Sandwich Structures with an Auxetic Honeycomb Core, *Composite Structures*, 260 (2021), 113256
- [8] Rzdolsky, L., Transient Engineering Creep of Materials under Various Fire Conditions, in: *Probability Based High Temperature Engineering*, Springer-Verlag, Berlin, Germany, 2017
- [9] Pešić, D. J., Raos, M. T., *Požari i Građevinske Konstrukcije* (in Serbian), Faculty of Occupational Safety, University of Niš, Niš, Serbia, 2017, p. 219
- [10] Stepinac, L., et al., Overview of Research on Fire Effects in RC Elements and Assessment of RC Structures After Fire, *Građevinar*, 73 (2021), 5, pp. 509-522
- [11] Fan, K., et al., Compressive Stress-Strain Relationship for Stressed Concrete at High Temperatures, *Fire Safety Journal*, 130 (2022), 103576
- [12] Moghadam, M. A., Izadifard, R., Evaluation of Shear Strength of Plain and Steel Fibrous Concrete at High Temperatures, *Construction and Building Materials*, 215 (2019), Aug., pp. 207-216
- [13] Wang, W., et al., An Investigation on Thermal Conductivity of Fly Ash Concrete after Elevated Temperature Exposure, *Construction and Building Materials*, 148 (2017), Sept., pp. 148-154
- [14] Durgun, M. Y., Sevinc, A. H., High Temperature Resistance of Concretes with GGBFS, Waste Glass Powder, and Colemanite Ore Wastes after Different Cooling Conditions, *Construction and Building Materials*, 196 (2019), Jan., pp. 66-81
- [15] Blagojevic, M., *Projektovanje Sistema za Dojavu Požara* (in Serbian), AGM knjiga, Faculty of Civil Engineering, Belgrade, 2018, p. 266
- [16] Blagojevic, M., et al., Comparative Analysis of Rules in Five Leading Standards for Smoke Detectors Sitting in the Presence of Ceiling Irregularity, *Transactions of the VSB*, 12 (2017), 2, pp. 23-29
- [17] ***, EN 54-14:2018 Fire detection and fire alarm system – Part 14: Guidelines for planning, design, installation, commissioning, use and maintenance, European Committee for Standardization (CEN), Brussels, Belgium, 2018
- [18] ***, DIN VDE 0833-2:2017 Alarm systems for fire, intrusion and hold up – Part 2: Requirements for fire alarm systems, VDE Verlag, Berlin, Germany, 2017
- [19] ***, BS 5839-1:2017 Fire detection and fire alarm systems for buildings. Code of practice for design, installation, commissioning and maintenance of systems in non-domestic premises, British Standards Institution, London, UK, 2017
- [20] ***, NFPA 72:2022 National Fire Alarm and Signaling Code, National Fire Protection Association, Quincy, Massachusetts, USA, 2022
- [21] ***, СП 484.1311500:2020 Системы противопожарной защиты. Системы пожарной сигнализации и автоматизация систем противопожарной защиты. Нормы и правила проектирования, ВНИИПО МЧС, Москва, Россия, 2020
- [22] McGrattan, K., et al., Fire Dynamics Simulator, Technical Reference Guide, Special Publication (NIST SP), National Institute of Standards and Technology, Gaithersburg, Md., USA, 2013
- [23] ***, UL 268:2016 UL Standard for Safety Smoke Detectors for Fire Alarm Systems, American National Standards Institute, Washington, USA, 2016